GeoHazards

MDPI

Article

Correlation of Ground Deformation Induced by the 6 February 2023 M7.8 and M7.5 Earthquakes in Turkey Inferred by Sentinel-2 and Critical Exposure in Gaziantep and Kahramanmaraş Cities

Ioannis Gkougkoustamos [1,*], Pavlos Krassakis [1,2], Georgia Kalogeropoulou [1] and Issaak Parcharidis [1]

[1] Department of Geography, Harokopio University of Athens, El. Venizelou 70, 17671 Athens, Greece; krassakis@certh.gr (P.K.); georgiakaloger22@gmail.com (G.K.); parchar@hua.gr (I.P.)
[2] Centre for Research & Technology Hellas (CERTH), 15125 Athens, Greece
* Correspondence: johnniegougos@gmail.com

Abstract: On 6 February 2023, an M7.8 devastating earthquake started rupturing the East Anatolian fault system in Turkey, resulting in intense shaking that lasted over a minute. A second earthquake of magnitude 7.5 struck near the city of Elbistan a few hours later. Both of these events are associated with the East Anatolian fault system. The earthquake sequence caused widespread damage and collapse of structures in densely populated areas throughout the Southern Turkey and Northern Syria regions and a very large number of human losses. This study focuses on the correlation of the ground deformation with the critical exposure of the infrastructures of Gaziantep and Kahramanmaraş cities. The estimation of the ground deformation of the affected area is achieved with the use of Copernicus Sentinel-2 products and the Normalized Cross Correlation algorithm (NCC) of image matching. The results of the East–West component show that specific sections of the region moved towards the East direction, reaching displacement measurements of 5.4 m, while other sections moved towards the West direction, reaching displacement measurements of 2.8 m. The results of the North–South component show that almost the whole affected area moved towards the North direction, with specific areas reaching displacements of 5.5 m, and a few exemptions, as some areas moved towards the South direction, with displacements reaching even 6.9 m. Regarding the cities of Kahramanmaraş and Gaziantep, their estimated movement direction is North-West and North-East, respectively, and is consistent with the movements of the Arabian and Anatolian Plates in which they are located. Important infrastructures of the study areas (education, museums, libraries, hospitals, monuments, airports, roads and railways) are superimposed on the findings, enabling us to detect the critical exposure rapidly.

Keywords: earthquake; Turkey; critical infrastructure exposure; correlation; Sentinel-2; ground deformation; normalized cross correlation (NCC); Gaziantep; Kahramanmaras

Citation: Gkougkoustamos, I.; Krassakis, P.; Kalogeropoulou, G.; Parcharidis, I. Correlation of Ground Deformation Induced by the 6 February 2023 M7.8 and M7.5 Earthquakes in Turkey Inferred by Sentinel-2 and Critical Exposure in Gaziantep and Kahramanmaraş Cities. *GeoHazards* **2023**, *4*, 267–285. https://doi.org/10.3390/geohazards4030015

Academic Editors: Paolo Boncio and Tiago Miguel Ferreira

Received: 2 April 2023
Revised: 16 June 2023
Accepted: 3 July 2023
Published: 6 July 2023

1. Introduction

Earthquakes are dangerous natural disasters and can cause natural, infrastructural and economic damage, as well as often claiming a large number of lives. The recording and monitoring of earthquakes is achieved thanks to modern instrumental seismology [1]. However, this does not provide immediate information regarding actual ground movement of the affected area and the impact of the earthquake. Field surveys are essentially the most effective and reliable method of retrieving this information. Earth Observation (EO) satellites are a non-invasive source of knowledge. The different types of sensors utilize different parts of the electromagnetic spectrum (optical and radar sensors) for observation. The processing of Synthetic Aperture Radar (SAR) images has proven to be a very reliable and precise tool for the measurement and observation of ground deformation caused by

earthquakes, with an accuracy of a few millimeters. The measurements provide the line-of-sight (LOS) component of the satellite towards the ground. If images with different orbits are utilized (ascending and descending orbits), then it is possible to retrieve the actual ground deformation in the East–West and Up–Down (uplift–subsidence) components. The limitation, however, is that it does not provide measurements for the North–South component [2]. Optical image-matching techniques are typically used to recover the two horizontal components of the 3D motion, with magnitudes reaching from a fraction of the image pixel size to several dozen pixels [3]. The goal of this study is the rapid computation and mapping of the ground displacement field induced by the M7.8 and M7.5 earthquakes that occurred on 6 February 2023 in Turkey and the correlation with the critical exposure of the infrastructures (education, museums, libraries, hospitals, monuments, airports, roads and railways) of Gaziantep and Kahramanmaraş cities. More specifically, the goal is the estimation of ground deformation in the locations of the critical infrastructures and the potential rapid identification of infrastructures that may be severely affected by ground displacement, using readily available satellite images. This process utilizes Copernicus Sentinel-2 products and employs the Normalized Cross Correlation (NCC) algorithm for estimation purposes. The results illustrate that this approach enables efficient emergency mapping, providing valuable insights for post-disaster assessment and response operations [4–7].

2. Tectonic Setting of the Broader Area

The Anatolian Plate is a tectonic plate that is separated from the Eurasian plate and the Arabian plate by the North Anatolian Fault Zone (NAFZ) and the East Anatolian Fault Zone (EAFZ), respectively (Figure 1). Most of Turkey is located on the Anatolian plate [8]. The Arabian Plate is a tectonic plate located in the Middle East of Asia, and it has been moving northward in geological history and colliding with the Eurasian Plate (Figure 1) [9]. The Sinai microplate is a triangular continental crustal block locked between the major Arabian and African plates and the Anatolian–Aegean microplate (Figure 1) [10]. The intersection between the Anatolian, the Arabian and the Sinai plates is a transform boundary, named Hatay Triple Junction, and it is the location where the 2023 destructive earthquakes occurred [11]. It was formed approximately 15 Ma and has migrated in a northeast direction along the East Anatolian fault to its present position.

The relative motions of the major tectonic plates (Arabian, Eurasian, African) and the smaller tectonic plates (Anatolian, Sinai) are responsible for the seismicity in Turkey. The geologic development of the region is a consequence of several first-order plate boundary interactions between these plates that include subduction, large-scale transform faulting, compressional mountain building and crustal extension. The closure of the Mediterranean Sea as the African and Arabian plates converge with the Eurasian plate causes westward motion of the Anatolian plate [12].

Furthermore, the northward motion of the Arabian plate appears to be transferred directly to the region of Turkey in the East Anatolian Fault. The Anatolian plate is decoupled from Eurasia along the North Anatolian fault. This different response in Eastern and Western Turkey to the collision of the Arabian plate may result from the different boundary conditions, the Hellenic arc forming a “free” boundary to the west and the Asian continent and oceanic lithosphere of the Black and Caspian Seas forming a resistant boundary to the north and east. The pattern of deformation indicates increasing motions toward the Hellenic arc, suggesting that the westward displacement and counterclockwise rotation of the Anatolian plate are driven both by “pushing” from the Arabian plate and by “pulling” or basal drag associated with the foundering African plate along the Hellenic subduction zone (Figure 1) [13]. Gaziantep is located on the Arabian Plate, while Kahramanmaraş is located on the Anatolian Plate.

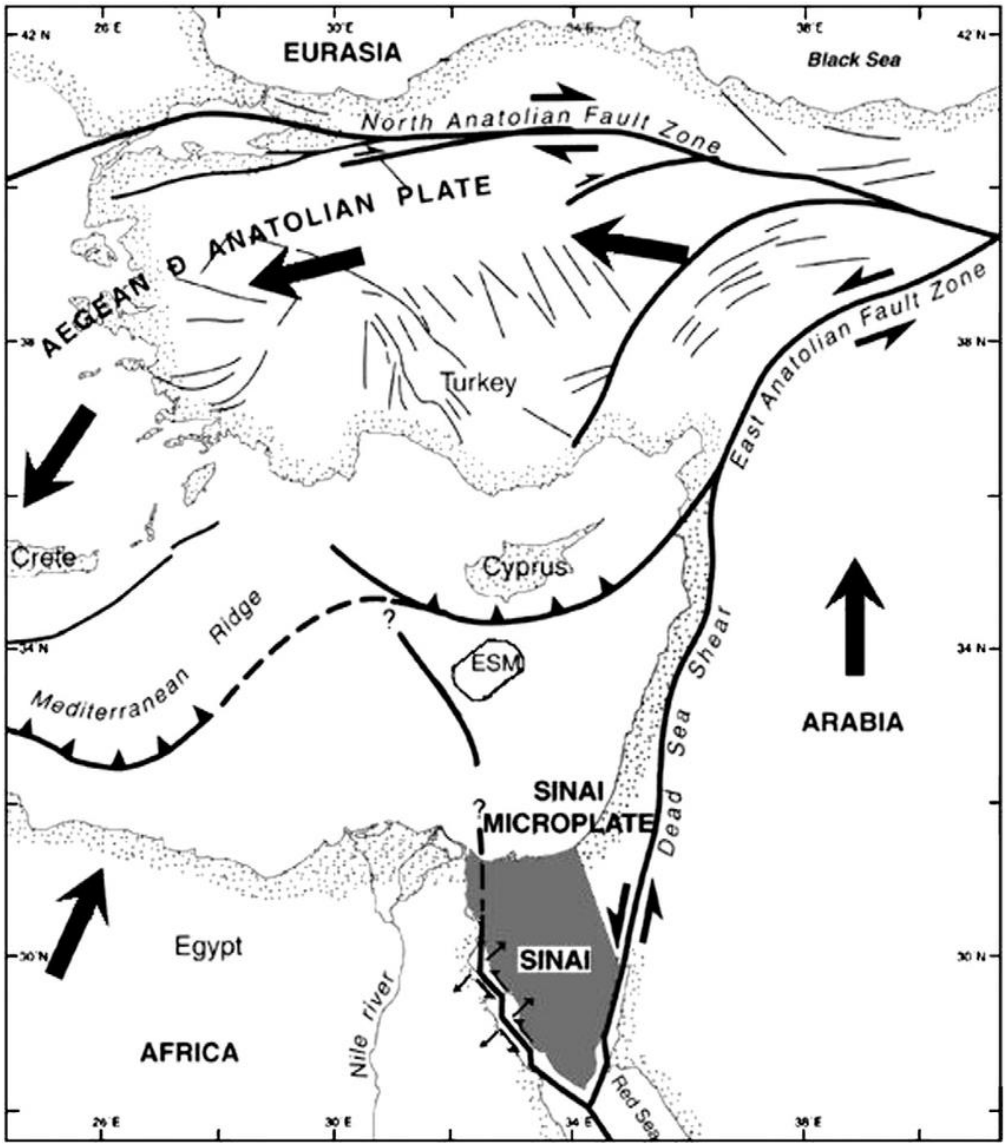

Figure 1. Map illustrating the Anatolian, Arabian, African and Sinai plates, their relative movement and the East and North Anatolian Fault Zones. Reprinted/adapted with permission from ref. [10].

Southern Turkey and Northern Syria have experienced significant and damaging earthquakes in the past. Aleppo (Syria) was devastated several times historically by large earthquakes, although the precise locations and magnitudes of these earthquakes can only be estimated. It was damaged by an estimated M7.1 earthquake in 1138, with 230,000 people killed [14], and an estimated M7.0 earthquake in 1822, with more than 10,000 lost lives [15]. The largest seismically documented earthquake on the East Anatolian fault was the M6.8 earthquake in 1905 that occurred in the central portion of the system. During the 20th century, seismicity along the East Anatolian fault had numerous M6 earthquakes, with most of the activity on the northern most section. In the last 25 years, the East Anatolia has been frequently affected by devastating earthquakes, such as the M6.3 Adana earthquake (27 June 1998), the M6.4 Bingöl earthquake (1 May 2003), the M7.2 Van earthquake (23 October 2011) and the M6.8 Elaziğ earthquake (24 January 2020) [16,17].

The Elevation map of the wider region (Figure 2) shows that the elevation ranges from 98.0 m to 2444.8 m. High elevation is prevalent in the west section of the region (west of Hassa, İslahiye and north of Bahçe and Andırın) and in the north section (north and northeast of Kahramanmaraş). The central section (northwest of Gaziantep) and the eastern section (where Gaziantep and Yavuzeli are located) are characterized by medium elevation,

and the rest of the region has generally low elevation (section from Kahramanmaraş to Deliosman and the western section near Düziçi).

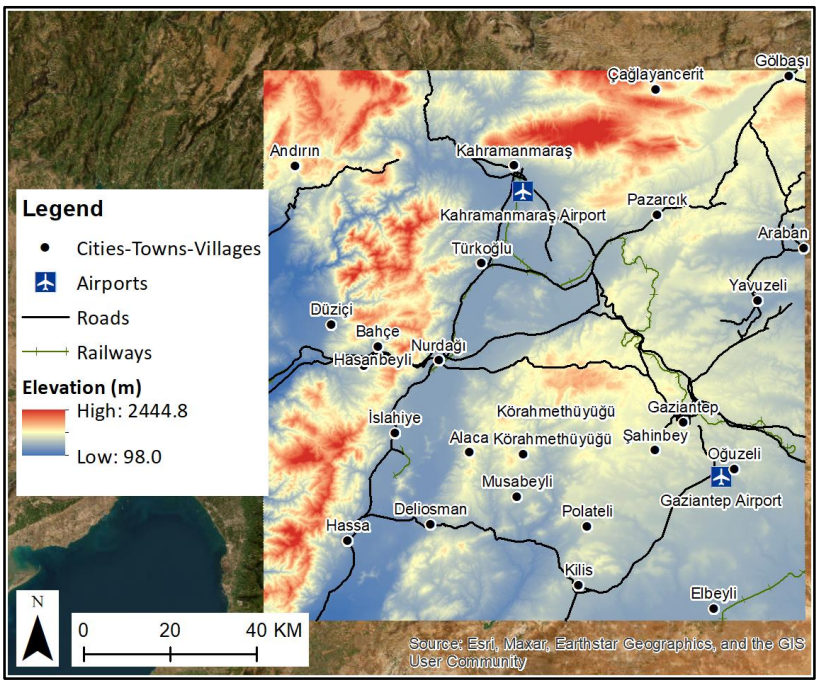

Figure 2. Elevation map of the wider region in meters. Lower elevation values are depicted in blue, while higher values are shown in red (Basemap source: ESRI).

The percent slope map of the wider region (Figure 3) shows a similar image to that of the elevation map. The percent slope values are higher in the sections where the elevation is high, especially in the areas north of Bahçe, west of Türkoğlu and west of Hassa. Lower-percent slope values are found in lower-elevated areas, such as the section from Kahramanmaraş to Deliosman and the southeast section north of Elbeyli.

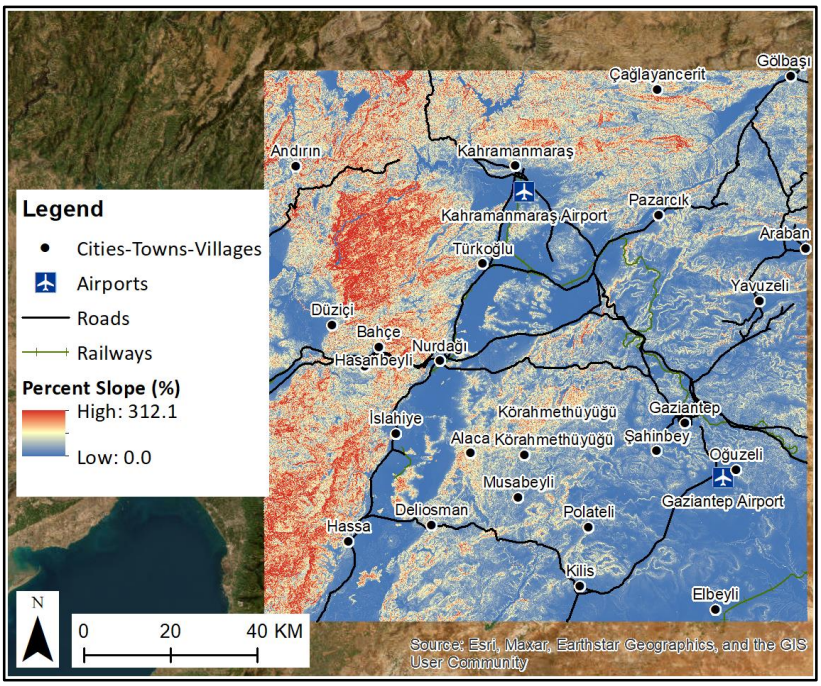

Figure 3. Percent slope map of the wider region in meters. Lower slope values are depicted in blue, while higher values are shown in red (Basemap source: ESRI).

3. Urban Setting of Gaziantep and Kahramanmaraş

Gaziantep (Figure 4) is a major city in south-central Turkey. It is the capital of the Gaziantep Province, and it is located approximately 185 km east of Adana and 97 km north of Aleppo, Syria, and situated on the Sajur River. As of the 2021 census, the Gaziantep province (metropolitan municipality) was home to 2,154,051 inhabitants. The Gaziantep Airport is located approximately 16 km southeast of the city [18].

Kahramanmaraş is a city in the Mediterranean region of Turkey and the administrative center of Kahramanmaraş province. It is situated at the edge of a fertile plain below Ahır Mountain, east-northeast of Adana. As of the 2021 census, the Kahramanmaraş metropolitan province was home to 1,177,436 inhabitants [18,19].

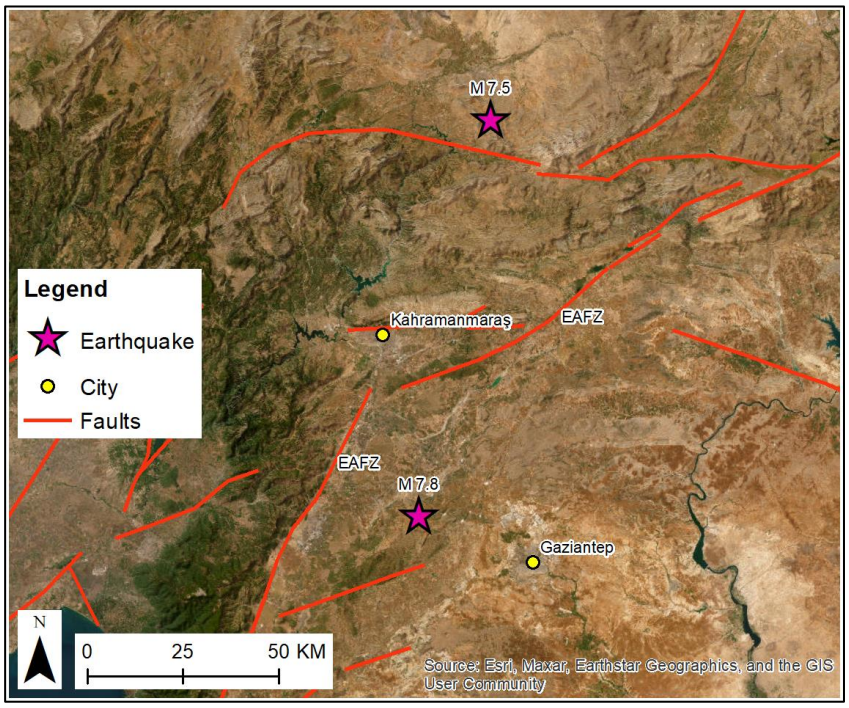

Figure 4. Gaziantep, Kahramanmaraş, the earthquake epicenters and the East Anatolian Fault Zone (EAFZ) location in Turkey [20] (Basemap source: ESRI).

The cities of Gaziantep and Kahramanmaraş are situated in close proximity to the East Anatolian Fault Zone (EAFZ), a significant tectonic feature in the region. The EAFZ is a major fault line that runs across eastern Anatolia in Turkey and is associated with seismic activity and frequent earthquakes [20]. Figure 4, mentioned in the statement, likely depicts a visual representation of the geographical relationship between the EAFZ, Gaziantep and Kahramanmaraş.

This figure provides a spatial perspective, showcasing the relative positions of the fault zone and the analyzed cities. Understanding the proximity and alignment of these cities with respect to the fault zone and the recent earthquake events is crucial for assessing and implementing appropriate measures for disaster preparedness and response [20].

According to the elevation map of Gaziantep city (Figure 5), the city's elevation varies between 765.1 and 1018.0 m. The map provides valuable information about the altitude distribution across different sections of the city. In particular, the eastern section of Gaziantep exhibits lower elevations compared to other parts of the city. This means that the land in the eastern area is situated at relatively lower heights above sea level. The lower elevation in this region might be attributed to natural topographical features, such as valleys or basins.

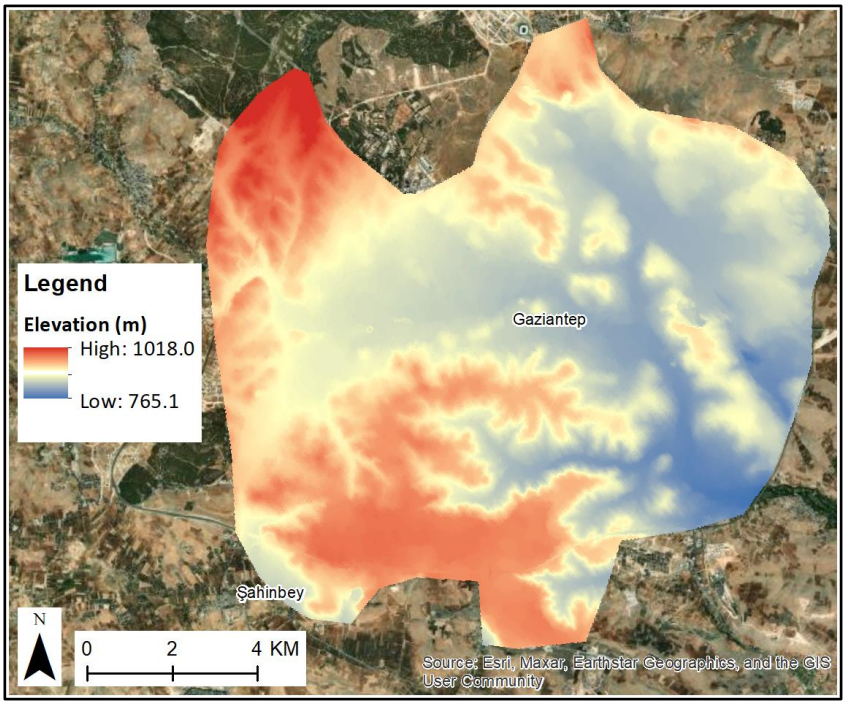

Figure 5. Elevation map of Gaziantep city. Lower elevation values are depicted in blue, while higher values are shown in red (Basemap source: ESRI).

The percent slope map of Gaziantep city (Figure 6) shows that the city has a generally flat topography, with a few exceptions in specific areas, especially in the south section, where the percent slope reaches 76.1%.

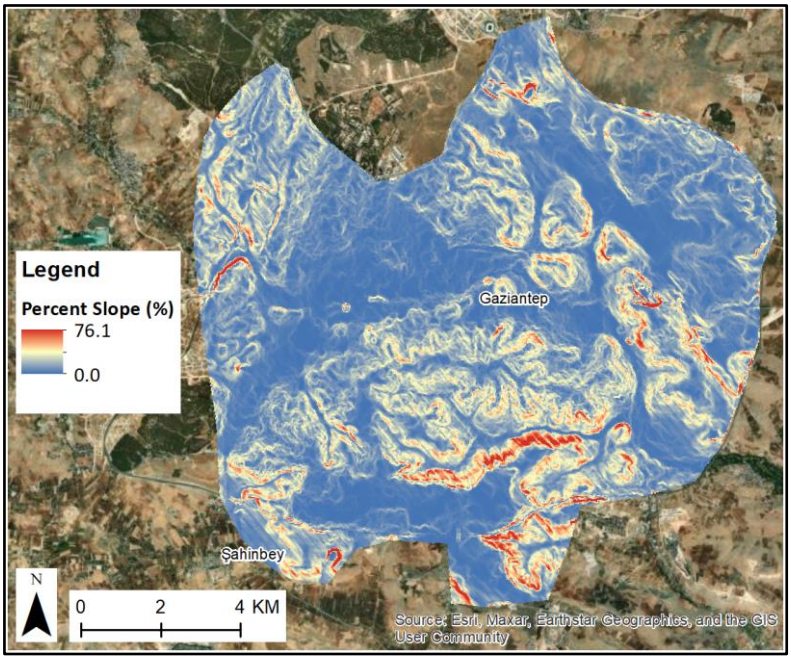

Figure 6. Percent slope map of Gaziantep city. Lower slope values are depicted in blue, while higher values are shown in red (Basemap source: ESRI).

The elevation map of Kahramanmaraş city (Figure 7) shows that the elevation ranges from 438.4 to 1052.0 m. The north section of the city has a high elevation, as it is located at the edge of Ahır Mountain, while the rest of the city has a lower elevation.

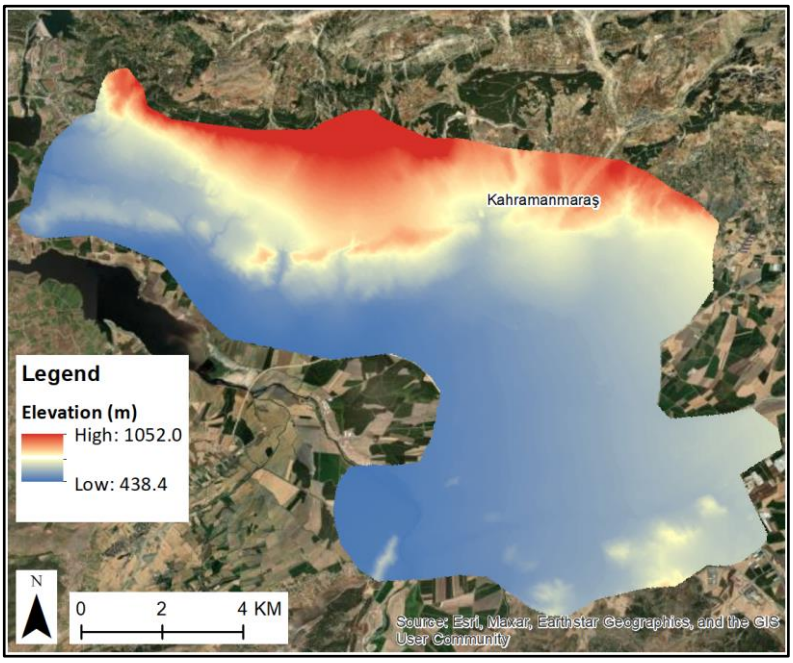

Figure 7. Elevation map of Kahramanmaraş city. Lower elevation values are depicted in blue, while higher values are shown in red (Basemap source: ESRI).

The percent slope map of Kahramanmaraş city (Figure 8) shows that the city has a varying topography. Most south sections have a flat topography, while the north sections are characterized by high-percent slope values that can reach 109.8%.

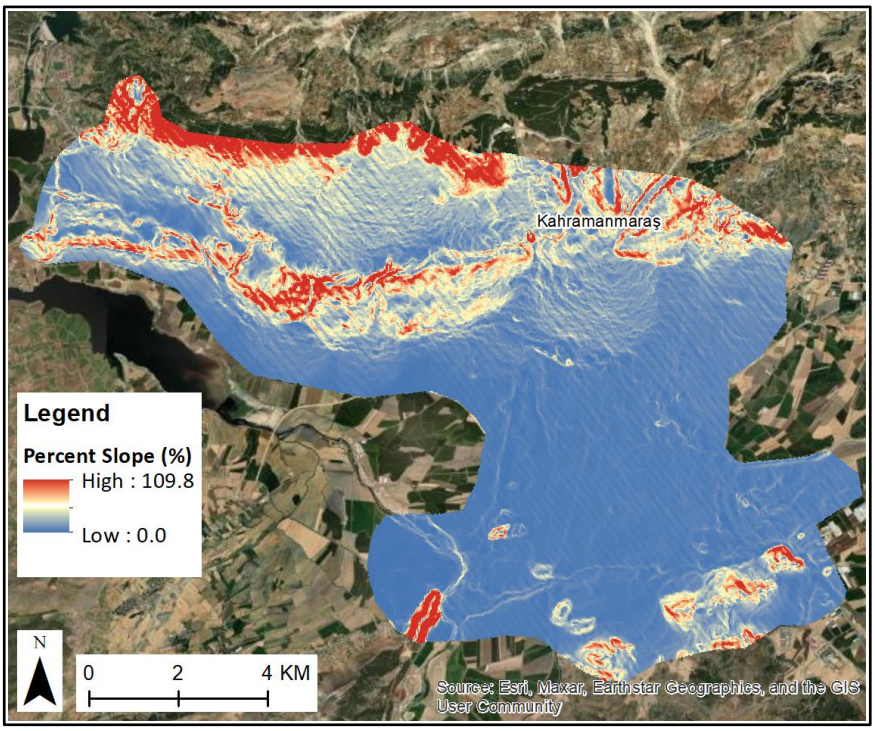

Figure 8. Percent slope map of Kahramanmaraş city. Lower slope values are depicted in blue, while higher values are shown in red (Basemap source: ESRI).

4. The Seismic Event

On 6 February 2023, at 01:17 UTC, an M7.8 earthquake started rupturing the East Anatolian fault system (Hatay Triple Junction), 33 km north-west of Gaziantep and 44 km

south of Kahramanmaraş. A few hours later, a magnitude 7.5 event occurred on a nearby branch of the fault system that trends east to west (Figure 4). This caused strong ground shaking [17]. The earthquake sequence caused widespread damage and collapse of structures in populated areas throughout the Southern Turkey and Northern Syria regions and a very large number of deaths. Further infrastructure damages include deformation and destruction of segments of the road network, deformation of railways, breakage of irrigation channels, etc. Slides and rockfalls were triggered, and the mobilized material was accumulated in adjacent parts of the road network, and in some sites, there was damage to adjacent buildings, especially in the mountainous parts and mountainous villages of the earthquake-affected area. In addition, liquefaction phenomena were observed, including ejection of liquefied material from soil cracks, sand boils as well as hydrological anomalies, such as the covering of large areas of the region by water due to the groundwater level rising.

Landslides and liquefaction phenomena were also observed in many sites characterized by high or critically high susceptibility. A tsunami of moderate intensity was also reported and recorded offshore northeastern Cyprus. It is worth mentioning that coastal inundation was also reported in the coastal area of İskenderun and attributed to coastal subsidence [16].

Additionally, 16 earthquakes occurred in the area in the period 25 January 2023 to 9 February 2023. These earthquakes are located near the major earthquakes and are higher than M5.0 [21] (Table 1).

Table 1. List of earthquakes in the wider region from 25 January 2023 to 9 February 2023 [21].

Earthquake	Date	Magnitude
1	6 February 2023	5.1
2	6 February 2023	5.6
3	6 February 2023	6.7
4	6 February 2023	5.0
5	6 February 2023	5.2
6	6 February 2023	5.7
7	6 February 2023	5.3
8	6 February 2023	5.1
9	6 February 2023	5.0
10	6 February 2023	5.0
11	6 February 2023	6.0
12	6 February 2023	5.0
13	7 February 2023	5.0
14	7 February 2023	5.5
15	7 February 2023	5.3
16	8 February 2023	5.1

5. Data and Methodology

5.1. Data

The Sentinel-2 mission, developed by the European Space Agency (ESA), is a constellation of two satellite units, Sentinel-2A and Sentinel-2B (launched in June 2014 and March 2017, respectively), that share the same orbital plane and feature a short repeat cycle of 5 days at the equator optimized to mitigate the impact of clouds in scientific studies and applications. Each satellite includes a multispectral instrument, with 13 spectral bands of

different resolutions (down to 10 m) and a swath width of 290 km. Since November 2015, the mission has been providing free images for global land observation [22].

The Level-2A products used in this study are composed of 100 × 100 km tiles (orthoimages in UTM/WGS84 projection). They are the result of various pre-processing steps, including the projection of the images in cartographic geometry using the Digital Elevation Model (DEM) Copernicus GLO-90m and atmospheric corrections (correction of Rayleigh scattering, of the absorbing and scattering effects of atmospheric gases, in particular ozone, oxygen and water vapor, and the correction of absorption and scattering due to aerosol particles). The products are resampled with a constant Ground Sampling Distance of 10, 20 and 60 m, depending on the native resolution of the different spectral bands [23,24].

In the context of this research, a total of eight Sentinel-2 Level-2A products (Table 2) from the ESA Copernicus Open Access HUB underwent processing:

Table 2. Copernicus Sentinel-2 products.

Product	Satellite	Date
Pre-event Image 1	Sentinel-2B	25 January 2023
Pre-event Image 2	Sentinel-2B	25 January 2023
Pre-event Image 3	Sentinel-2B	25 January2023
Pre-event Image 4	Sentinel-2B	25 January 2023
Post-event Image 1	Sentinel-2A	9 February 2023
Post-event Image 2	Sentinel-2A	9 February 2023
Post-event Image 3	Sentinel-2A	9 February 2023
Post-event Image 4	Sentinel-2A	9 February 2023

The images are selected as close to the date of the seismic event as possible, and it was verified that there was no snow covering the cities of Gaziantep and Kahramanmaraş on those specific dates, with data from the Meteostat Database [25,26].

Moreover, the Copernicus Emergency Management Service (EMS) was activated for this destructive earthquake. The Copernicus EMS provides information for emergency response in relation to different types of disasters, including meteorological hazards, geophysical hazards, deliberate and accidental man-made disasters and other humanitarian disasters, as well as prevention, preparedness, response and recovery activities. It consists of the Mapping Service and of the Early Warning System (floods), it has been an operational activity since 1 April 2012 and it is a fully operational service, as defined in Article 5 to the Copernicus Regulation [27]. The EMSR648 activation was utilized, and the locations and information for the critical infrastructures of the cities (education, museums, libraries, hospitals, monuments, airports, roads and railways) were retrieved.

Finally, a Digital Elevation Model (DEM) was utilized using FABDEM Version 1-2, where forests and buildings were removed from the Copernicus GLO 30 Digital Elevation Model (DEM). The data are available from the University of Bristol at 1 arc second grid spacing (approximately 30 m at the equator) for the globe [28].

5.2. Methodology

Pre-processing: The images were imported into the SNAP (9.0) software, and then each band was resampled at a resolution of 10 m. Then, two mosaics were generated, one from the pre-event image that covers the study area, and one from the post-event image that covers the same area. Band 4 (red visible) of each mosaic was extracted as a GeoTIFF file.

Main processing: The two files were imported in Correlation Image Analysis Software (CIAS, v.23), a free image correlation software that computes displacements between two single-band images (pre-event and post-event). A grid of points was generated over the study area, and then for each one, the Normalized Cross-Correlation (NCC) algorithm

was applied. The NCC algorithm corresponds pixel groups between two images based on their resemblance. Initially, a frame of pixels (Reference Block) was extracted from the pre-event image. This frame was then searched in a larger area of the post-event image (Search Area). After searching it in the form of a sliding window, the position of the frame in the Search Area that resembles the original frame the most is the position that this original frame has been shifted to (Figure 9) [4–7]. The processing parameters defined for the study area were: Reference Block: 100 pixels, Search Area Size: 150 pixels, Grid Distance: 1000 m.

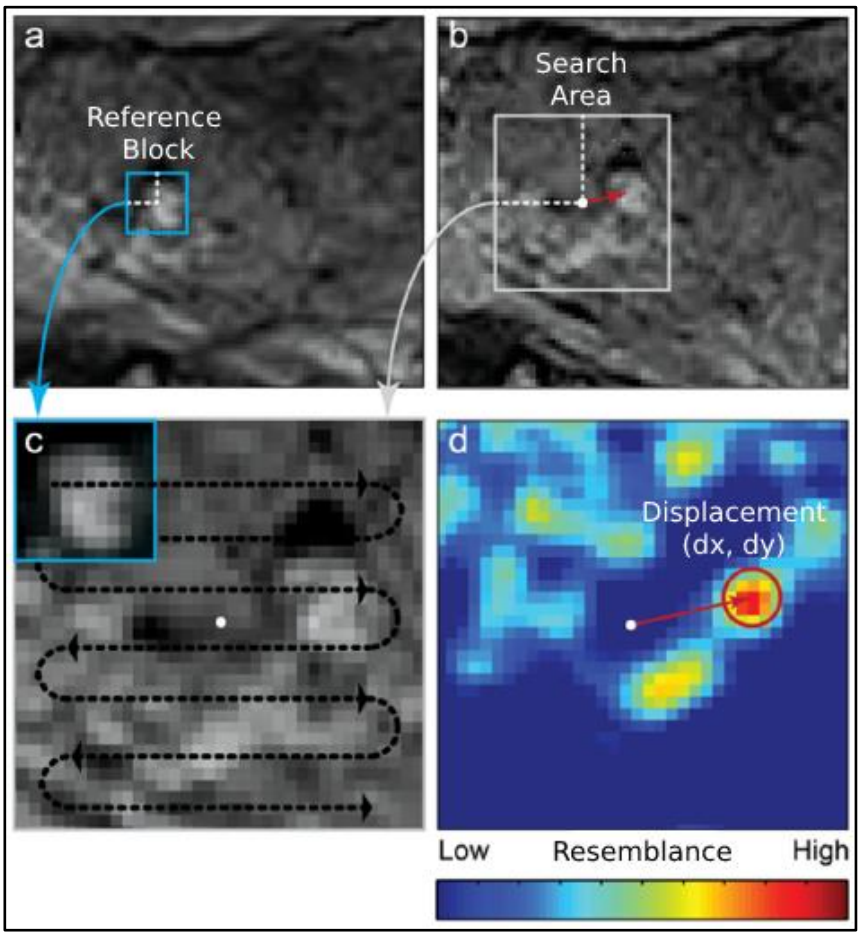

Figure 9. Schematic illustration of the region-based image-matching algorithm using Normalized Cross Correlation (NCC): (**a**) Reference Block, (**b**) Search Area, (**c**) Evaluation of the resemblance of the Reference Block in a sliding window fashion inside the Search Area and (**d**) Estimation of the displacement (dx, dy) of the Reference Block based on the maximum resemblance [3]. The arrows illustrate the relation between the Reference Block and Search Area. Specifically, the evaluation of the Reference Block resemblance is calculated inside the Search Area window.

The result was an ASCII file with coordinates of the centers of the frames searched (X, Y), the horizontal and vertical shifting of the frames (dx, dy), the total length and direction of the displacements, the degree of similarity between the pre-event frames and the post-event frames (maximum correlation coefficient) and the average similarity of the original frames to their surrounding areas (average correlation coefficient).

Post-processing: The file was imported into ArcMAP (10.4) software, and a mask of areas without snow cover was applied in the measurements. The snow mask is already provided in the atmospherically corrected Sentinel-2 products that were utilized; therefore, there are no measurements in areas that were covered in snow either in the pre-event images or the post-event images. This mask was applied in order to eliminate any possible miscalculations of ground deformation due to snow cover. The study area is equal to 16,172.4 km^2, the area with snow cover is equal to 5148.65 km^2 and the area with no

snow cover where the measurements were estimated is equal to 11,023.75 km^2. Then, two interpolation methods were executed, one for the dx estimations and one for the dy estimations. This resulted in two raster layers that indicate the displacement in the East–West and North–South components, respectively, for the wider affected area. For Gaziantep and Kahramanmaraş the measurements were visualized with the use of vectors.

6. Results

The results are visualized in four maps, showing the displacement in the East–West and North–South components for the wider affected area, and with the use of vectors for Gaziantep and Kahramanmaraş cities and their infrastructure exposure. For the areas that were covered by snow in the pre- and post-event images, displacement could not be estimated.

6.1. East–West Displacement

The results for the East−West component depict a clear difference in the displacement of the wider affected region due to the earthquake. The section of the study area south of Pazarcık city and east of İslahiye city moved towards the East direction, with a displacement range between 0.0 and 2.0 m. Notably, in the areas near Pazarcık city, the displacement length was even higher, reaching 5.4 m (Figure 10). The sections north of Türkoğlu and west of Nurdağı moved towards the west direction, and in some areas reached displacements of 2.8 m. Along the EAFZ, the difference in the region movement is abrupt, as the section west of the EAFZ moved towards the west, and the section east of the EAFZ moved towards the east.

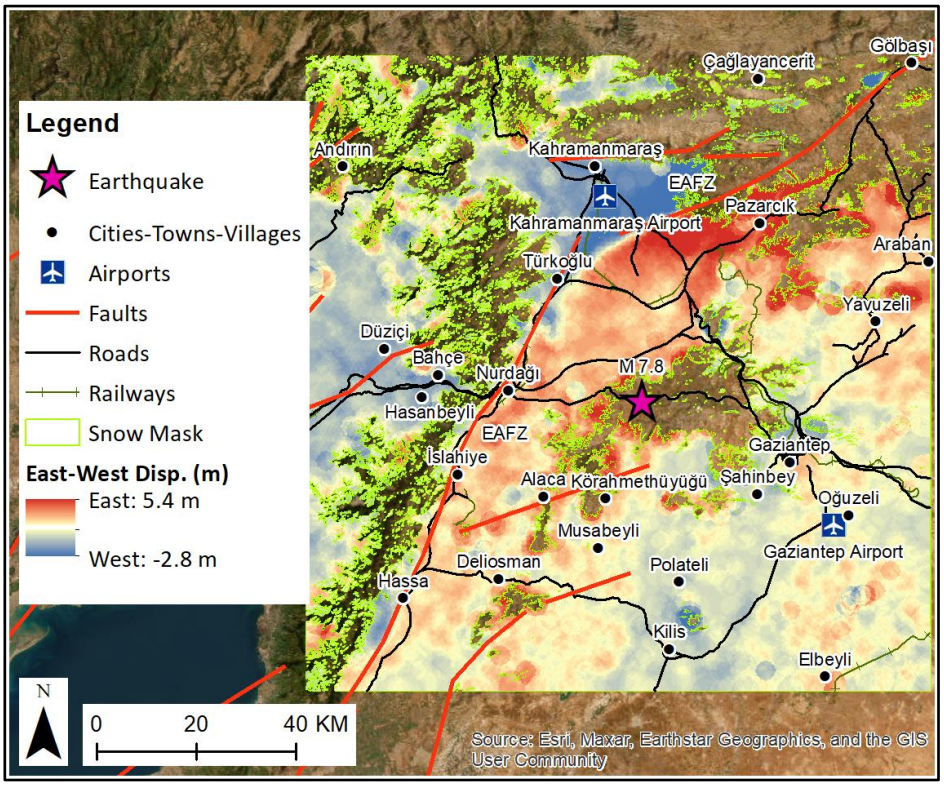

Figure 10. Displacement in the East−West component for the wider affected area (East: red values, West: blue values, Basemap source: ESRI).

In total, 190.51 km^2 of the study area moved towards the east, with displacement between 2.0 and 5.4 m, 8162.28 km^2 moved towards the east, with displacement less than 2.0 m, 2659.55 km^2 moved towards the west, with displacement less than 2.0 m and 11.40 km^2 moved towards the west, with displacement between 2.0 m and 2.8 m (Table 3).

Table 3. Displacement in the East–West component for the wider affected area.

Direction	Displacement (m)	Area (km^2)
East	2.0−5.4	190.51
East	0.0−2.0	8162.28
West	0.0−2.0	2659.55
West	2.0−2.8	11.40

6.2. North–South Displacement

Regarding the North–South component, the sections between the cities of Hassa and Elbeyli and between the cities of Hassa and Pazarcık moved towards the north direction, with displacement ranging between 2.0 and 5.5 m (Figure 11). The rest of the study area moved towards the north direction as well but with displacement less than 2.0 m. Some exceptions can be observed in the map, however, with blue color near the edges of the snow mask (areas near Andırın, Bahçe, Hassa, south-east of Kahramanmaraş and north-east of Gaziantep), where the ground displacement has a south direction. The maximum displacement observed towards the south direction is equal to 6.9 m. Similar to the East–West component, an abrupt difference in displacement can be observed along the EAFZ.

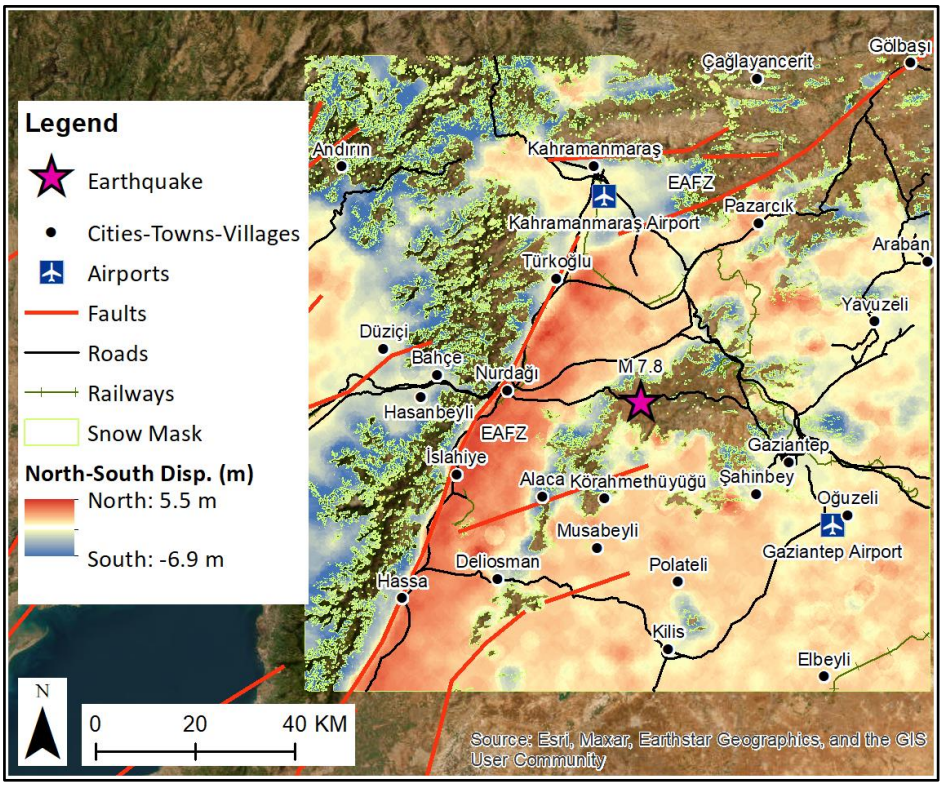

Figure 11. Displacement in the North−South component for the wider affected area (North: red values, South: blue values, Basemap source: ESRI).

In total, 5293.02 km^2 of the study area moved towards the north, with displacement between 2.0 and 5.5 m, 4315.48 km^2 moved towards the north, with displacement less than 2.0 m, 1075.97 km^2 moved towards the south, with displacement less than 2.0 m and 339.27 km^2 moved towards the south, with displacement between 2.0 m and 6.9 m (Table 4).

Table 4. Displacement in the North–South component for the wider affected area.

Direction	Displacement (m)	Area (km^2)
North	2.0−5.5	5293.02
North	0.0−2.0	4315.48
South	0.0−2.0	1075.97
South	2.0−6.9	339.27

6.3. Displacement and Critical Exposure in Gaziantep City

Gaziantep has a total of 4 museums, libraries, 195 educational buildings, 6 hospitals and 2 monuments. The displacement shows it primarily moved towards the North and North-East direction. However, the movement is not uniform in the whole city, as there are some areas with measurements in close proximity that show difference in the East–West component. Those areas are mainly located in the center, south, west and north-west sections of the city, as pairs of adjacent measurements show north-west and north-east movements, respectively. This shows the locations of possible surface ruptures or distortions, and they are locations that are considered in the correlation. Out of the total 144 measurements, 116 measurements show displacement less than 2.0 m, 26 measurements show displacement ranging from 2.1 m to 4.0 m and 2 measurements show displacement ranging from 4.1 m to 6.3 m (Figure 12).

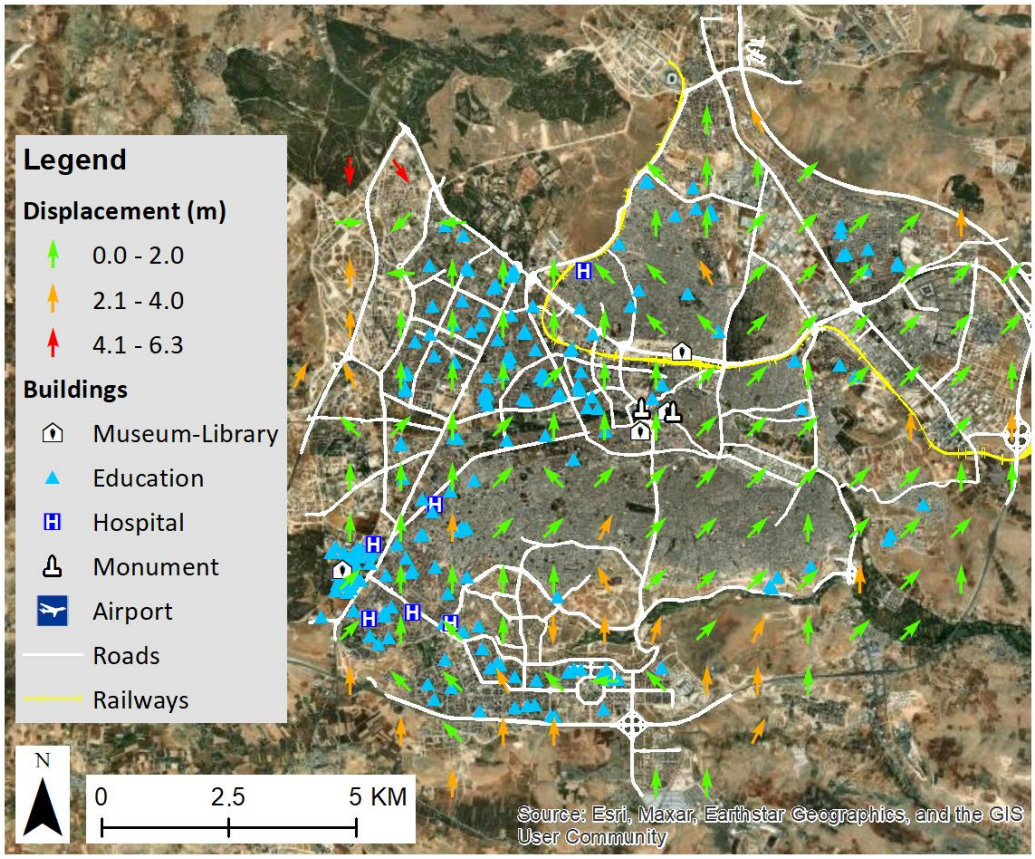

Figure 12. Displacement vectors and infrastructure exposure for Gaziantep City (Basemap source: ESRI).

From the correlation of the ground displacement with the critical infrastructures, it is clear that all of the important infrastructures are located in areas with displacement less than 2.0 m, with the exception of 15 educational buildings and 1 hospital, which are located in areas with displacement between 2.1 m and 4.0 m. Moreover, there are three educational buildings that are between adjacent measurements with different di-

rections of movement (possible surface ruptures). After comparison with the elevation map (Figure 5) and the percent slope map of Gaziantep (Figure 6), a correlation is observed between the high displacement measurements and high elevation and percent slope. Specifically, all the measurements that are higher than 2.1 m are located in areas where the elevation and percent slope values are also high and could be the locations of possible earthquake-induced landslides.

Based on the data from EMSR648, which provides information on the damage caused by the earthquake event in Gaziantep city, it is reported that a total of 19 buildings were possibly damaged, 9 buildings were confirmed to be damaged, and 44 buildings were completely destroyed (as indicated in Figure 13). These affected buildings primarily consist of residential structures, with a few remaining unclassified in terms of their usage.

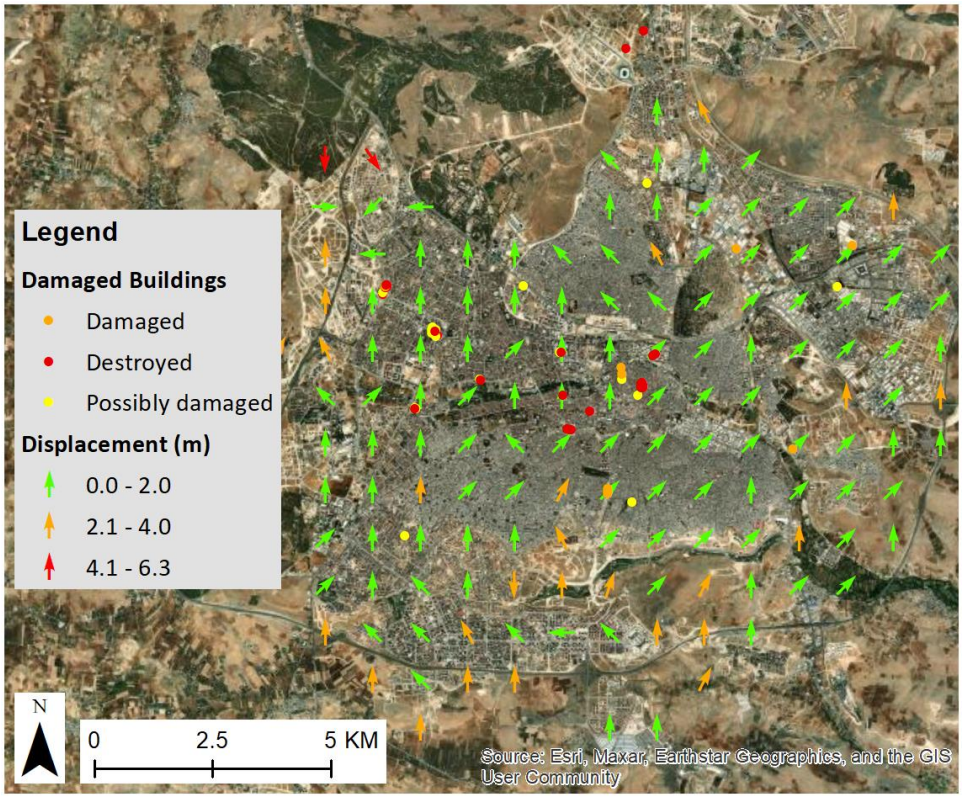

Figure 13. Damage map of Gaziantep City (source: Copernicus EMSR648, Basemap source: ESRI).

It is noteworthy that despite the significant impact on buildings, no critical infrastructures in the city were reported as damaged or destroyed. Critical infrastructures typically include essential facilities, such as hospitals, power plants, transportation hubs and communication networks, that are vital for the functioning of a city. By comparing the damage map, which likely illustrates the spatial distribution of the damaged and destroyed buildings, with the displacement map of Gaziantep, it is inferred that the affected buildings are not situated in areas where high levels of displacement, specifically exceeding 2.1 m, were observed. Furthermore, no damaged buildings are observed in locations of possible surface ruptures (location with adjacent measurements showing different directions of movement). Therefore, in this case, the ground displacement does not significantly affect the infrastructures, and the damage is probably only a result of the ground shaking.

6.4. Displacement and Critical Exposure in Kahramanmaraş City

Kahramanmaraş has a total of 13 museums, libraries, 105 educational buildings, 9 hospitals and 1 monument. The displacement shows that the whole city moved towards the North-West direction. Out of the total 123 measurements, 11 measurements show displacement less than 1.5 m, and 112 measurements show displacement ranging from

1.6 m to 2.8 m (Figure 14). From the correlation of the ground displacement with the critical infrastructures, it is concluded that eight educational buildings and 4 museums and libraries are located in areas with displacement less than 1.5 m. The rest of the critical infrastructures are located in areas with displacement between 1.6 m and 2.8 m.

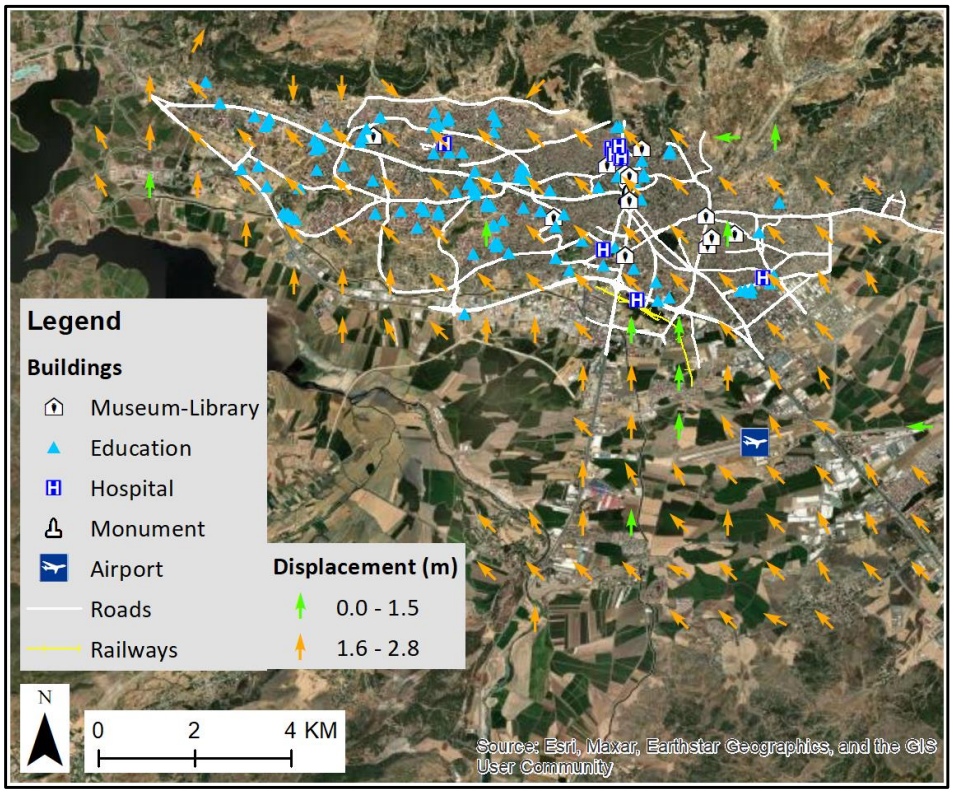

Figure 14. Displacement vectors and infrastructure exposure for Kahramanmaraş City (Basemap source: ESRI).

After comparison with the elevation map (Figure 7) and the percent slope map of Kahramanmaraş (Figure 8), it is concluded in this case that there is not a correlation between the displacement measurements and the elevation or percent slope of the area, as the majority of measurements show a North-West direction and length between 1.6 m and 2.8 m, despite the changes in elevation and percent slope. The only exemption is that four measurements in the northern part of the city have a South direction, and since this area has high elevation and percent slope (edge of mount Ahir), this could be the location of possible landslides induced by the earthquakes.

According to the EMSR648 data, in Kahramanmaraş city, 456 buildings (Figure 15) were possibly damaged, 185 buildings were damaged and 286 buildings were destroyed. Regarding the critical infrastructures of the city, four educational buildings were possibly damaged, and one educational building was damaged. The affected buildings are mainly observed in the central section of the city. Comparing the damage map with the displacement of Kahramanmaraş, we observe that the majority of damaged and destroyed buildings, including the abovementioned educational buildings, are in areas where displacement is high (>1.6 m).

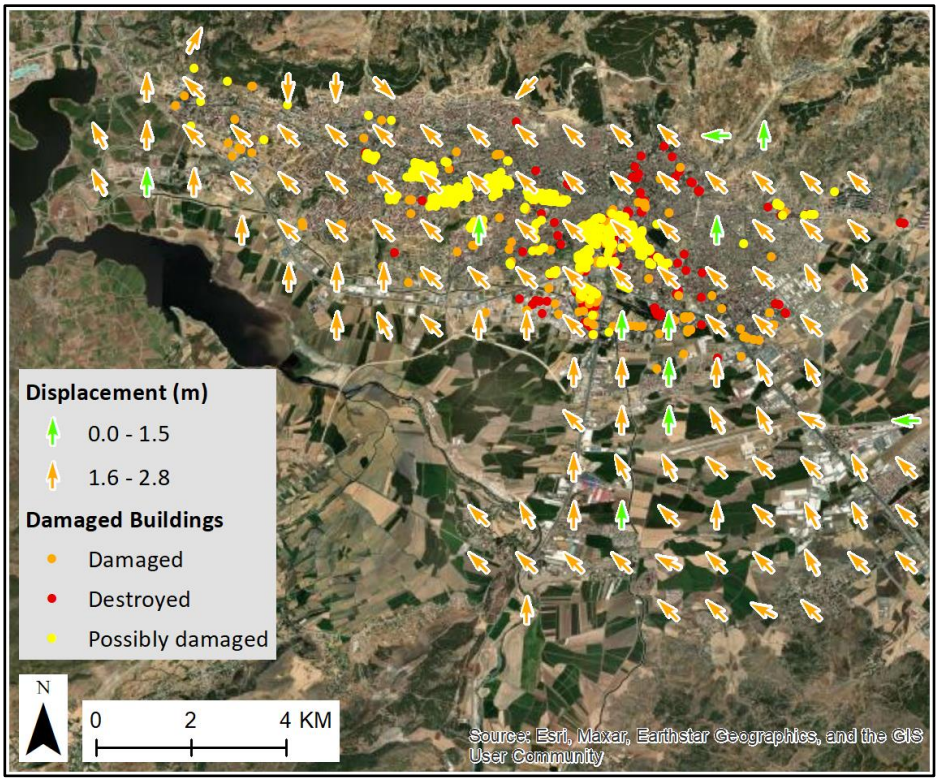

Figure 15. Damage map of Kahramanmaraş City (source: Copernicus EMSR648, Basemap source: ESRI).

7. Discussion and Conclusions

The subject of this study was the rapid computation and mapping of the ground displacement field due to the strong M7.8 and M7.5 earthquakes in Turkey and the correlation with the critical exposure of the infrastructures (education, museums, libraries, hospitals, monuments, airports, roads and railways) of Gaziantep and Kahramanmaraş cities, with the use of medium-resolution optical satellite images, specifically Sentinel-2, and the Normalized Cross-Correlation (NCC) method of image matching. According to the measurements regarding the East–West component, a clear difference is observed in the displacement of the wider affected region due to the earthquake. A large section south of Pazarcık city and east of İslahiye city moved towards the East direction and it reached 5.4 m in areas near Pazarcık. Instead, the sections north of Türkoğlu and west of Nurdağı moved towards the West direction, reaching displacements of 2.8 m in some regions. A clear difference in region movement can be observed along the EAFZ, as the section west of the EAFZ moved towards the West, and the section east of the EAFZ moved towards the East. Regarding the North–South component, almost the whole study area moved towards the North direction, with specific areas reaching displacements of 5.5 m, and with a few exemptions observed near the edges of the snow mask, as some areas moved towards the South direction (areas near Andırın, Bahçe, Hassa, south-east of Kahramanmaraş and north-east of Gaziantep). The maximum South direction displacement observed is equal to 6.9 m. Similar to the East–West component, an abrupt difference in displacement can observed along the EAFZ.

Comparing these results with the reports of ForM@Ter [29] and CEDA [30], similar conclusions are observed in the East-West displacement field. Specifically, both reports show the difference in region movement along the EAFZ (section west of EAFZ moving towards the West direction, section east of EAFZ moving towards the East direction). Regarding the displacement values in the EAFZ, the ForM@Ter report [29] shows maximum displacements of 9.6 m and 8.1 m in the East and West directions, respectively, while CEDA [30] shows maximum displacements of 4 m in both East and West directions. In the case of the North–South component, however, both reports [29,30] show a difference

in region movement along the EAFZ (section west of EAFZ moving towards the South direction, section east of EAFZ moving towards the North direction), which is different from this study's result that shows a general movement of the region towards the North direction, with only a few specific locations moving towards the South direction. Since both reports used the same images that were used in this study (Sentinel-2: 25 January 2023 and 9 February 2023), the difference in the North–South component could be attributed to the different processing methods and software of the multispectral images (GDM-OPT-ETQ service was used in the ForM@Ter report [29] and ENVI COSI-Corr in the CEDA report [30]), as well as different processing parameters and processing iterations. Possible actions for reducing the uncertainty of the North–South component could be more processing iterations with different combinations of Reference Block and Search Area window sizes. Moreover, a more precise coregistration could be applied to the Sentinel-2 products before the main processing, in case there are possible misalignments of the images. Regarding the displacement values in the EAFZ, the ForM@Ter report [29] shows maximum displacements of 11 m and 18.6 m in the North and South directions, respectively, while CEDA [30] shows maximum displacements of 4 m in both North and South directions.

The displacement vectors for Gaziantep show that it primarily moved towards the North and North-East direction, with the majority of measurements showing displacement less than 2.0 m, and the rest of the measurements showing displacement ranging from 2.1 m to 4.0 m and from 4.1 m to 6.3 m. Regarding the critical infrastructure exposure of the city, all the important infrastructures are located in areas with displacement less than 2.0 m, with the exemption of 15 educational buildings and 1 hospital, which are located in areas with displacement between 2.1 and 4.0 m. A correlation is observed with the elevation and percent slope of the city, as all the measurements that are higher than 2.1 m are located in areas where the elevation and percent slope values are also high. Those could be the locations of possible earthquake-induced landslides. Moreover, specific locations of probable surface ruptures were identified.

The displacement vectors for Kahramanmaraş essentially show that the whole city moved towards the North-West direction, with 11 measurements showing displacement less than 1.5 m and 112 measurements showing displacement ranging from 1.6 m to 2.8 m. Therefore, the movements of the two cities are consistent with the relative movements of the Arabian and Anatolian Plates in which they are located. Regarding the critical infrastructure exposure of the city, eight educational buildings and four museums and libraries are located in areas with displacement less than 1.5 m, and the rest of the critical infrastructures are located in areas with displacement between 1.6 m and 2.8 m. In Kahramanmaraş, there is not a clear correlation between the displacement measurements and the elevation or percent slope. There is an exemption; however, in the north part of the city, where four measurements have a South direction, and since this area has high elevation and percent slope (edge of mount Ahir), the measurements are possibly showing the location of earthquake-induced landslides.

Regarding the comparison of the EMSR648 damage map with the displacement in Gaziantep city, it is concluded that no critical infrastructures were damaged or destroyed in areas where displacement is high (>2.1 m). In the case of Kahramanmaraş, however, the comparison of the EMSR648 damage map with the displacement shows that there were four possibly damaged educational buildings and one damaged educational building located in areas with high displacement (>1.6 m).

It is important to note that damage and destruction of buildings and infrastructures are mainly a result of the ground shaking during an earthquake. Additionally, the effects of an earthquake on infrastructures are a result of their maintenance, material quality, construction methods, comprehensive structural and earthquake design studies, and consideration of geological and geomorphological features of the wider area. This study, however, focuses specifically on the production of very fast preliminary information regarding ground displacement, which can be estimated for very large areas with readily available multispectral images, the identification of possible surface ruptures in areas where the measurements do

not show similar movement directions and the identification of specific locations where damage, destruction and human casualties are highly possible.

The use of readily available multispectral images only, for the study of such a destructive event, has two limitations: (A) Specific locations in the wider region of the study area are covered by snow; therefore, there are no measurements in those specific locations. This is an important limitation in cases of rapid mapping. However the results of the methodology used are estimated only in areas without snow cover and, therefore, they represent ground movement not affected by snow. (B) Finally, it is impossible to derive vertical displacement of the ground without the processing of SAR images. The vertical component is very important, since subsidence or uplift of the ground can cause severe damage in populated areas. Therefore, a more complete approach would consist of the processing of both multispectral and SAR images, in order to estimate deformation in the East–West, North–South and Up–Down components, to examine their relative displacement and their relation to critical infrastructures.

Author Contributions: Conceptualization, I.P., I.G. and P.K.; methodology, I.G. and P.K.; validation, I.P., I.G. and P.K.; formal analysis, I.P., I.G. and P.K.; investigation, I.P., I.G. and P.K.; resources, I.P., I.G., P.K. and G.K.; data curation, I.P., I.G., P.K. and G.K.; writing—original draft preparation, I.P., I.G., P.K. and G.K.; writing—review and editing, I.P., I.G. and P.K.; visualization, I.P., I.G. and P.K.; supervision, I.P. All authors have read and agreed to the published version of the manuscript.

Funding: This research received no external funding.

Data Availability Statement: Data available upon request.

Acknowledgments: Maps and diagrams throughout this work were created using ArcGIS® software by Esri. ArcGIS® and ArcMap™ are the intellectual property of Esri and are used herein under license. Copyright © Esri. All rights reserved. For more information about Esri® software, please visit https://www.esri.com/en-us/home (accessed on 2 July 2023). The authors are grateful to the European Space Agency (ESA) who provided Sentinel-2 products. The authors would also like to thank the reviewers for providing useful suggestions that enhance the manuscript's quality. The image matching code used for this study (Correlation Image Analysis Software, CIAS) is available from: https://www.mn.uio.no/geo/english/research/projects/icemass/cias/ (accessed on 2 July 2023).

Conflicts of Interest: The authors declare no conflict of interest.

Data Sources: Google Earth Pro Software. ESA Copernicus Open Access HUB. Available online: https://scihub.copernicus.eu (accessed on 2 July 2023). Copernicus Emergency Management Service—Mapping. Available Online: https://emergency.copernicus.eu/mapping/list-of-components/EMSR648 (accessed on 2 July 2023). University of BRISTOL. FABDEM V1-2. Available online: https://data.bris.ac.uk/data/dataset/s5hqmjcdj8yo2ibzi9b4ew3sn (accessed on 2 July 2023).

References

1. U.S. Geological Survey. The Science of Earthquakes. Available online: https://www.usgs.gov/programs/earthquake-hazards/science-earthquakes (accessed on 3 March 2023).
2. Ferretti, A. *Satellite InSAR Data: Reservoir Monitoring from Space*; EAGE Publications: Kosterijland, The Netherlands, 2014. [CrossRef]
3. Stumpf, A.; Malet, J.P.; Puissant, A.; Travelletti, J. *Monitoring of Earth Surface Motion and Geomorphologic Processes by Optical Image Correlation. Land Surface Remote Sensing*; Elsevier: Amsterdam, The Netherlands, 2016; pp. 147–190, ISBN 9781785481055. [CrossRef]
4. UiO Department of Geosciences. Image Correlation Software CIAS. Available online: http://www.mn.uio.no/geo/english/research/projects/icemass/cias/ (accessed on 5 March 2023).
5. Debella-Gilo, M.; Kääb, A. Sub-pixel precision image matching for measuring surface displacements on mass movements using normalized cross-correlation. *Remote Sens. Environ.* **2011**, *115*, 130–142. [CrossRef]
6. Heid, T.; Kääb, A. Evaluation of existing image matching methods for deriving glacier surface displacements globally from optical satellite imagery. *Remote Sens. Environ.* **2012**, *118*, 339–355. [CrossRef]
7. Kääb, A.; Vollmer, M. Surface geometry, thickness changes and flow fields on creeping mountain permafrost: Automatic extraction by digital image analysis. *Permafr. Periglac. Process.* **2000**, *11*, 315–326. [CrossRef]

8. Smithsonian Institution. 7.8-Magnitude Earthquake Felt 'Like the Apocalypse' in Turkey and Syria. Available online: https://www.smithsonianmag.com/smart-news/78-magnitude-earthquake-felt-like-the-apocalypse-in-turkey-and-syria-180981587/ (accessed on 3 March 2023).
9. African/Arabian Tectonic Plates. The Arabian Plate. Available online: https://africa-arabia-plate.weebly.com/arabian-plate.html (accessed on 4 March 2023).
10. Mascle, J.; Benkhelil, J.; Bellaiche, G.; Zitter, T.; Woodside, J.; Loncke, L. Prismed II Scientific Party, Marine geologic evidence for a Levantine–Sinai plate, a new piece of the Mediterranean puzzle. *Geology* **2000**, *28*, 779–782. [CrossRef]
11. Mahmoud, Y.; Masson, F.; Meghraoui, M.; Cakir, Z.; Alchalbi, A.; Yavasoglu, H.; Yönlü, O.; Daoud, M.; Ergintav, S.; Inan, S. Kinematic study at the junction of the East Anatolian fault and the Dead Sea fault from GPS measurements. *J. Geo-Dyn.* **2013**, *67*, 30–39. [CrossRef]
12. USGS. The 2023 Kahramanmaras, Turkey Earthquake Sequence. Available online: https://earthquake.usgs.gov/storymap/index-turkey2023.html?utm_source=hootsuite (accessed on 5 March 2023).
13. Reilinger, R.E.; McClusky, S.C.; Oral, M.B.; King, R.W.; Toksoz, M.N.; Barka, A.A.; Kinik, I.; Lenk, O.; Sanli, I. Global Posi-tioning System measurements of present-day crustal movements in the Arabia-Africa-Eurasia plate collision zone. *J. Geophys. Res.* **1997**, *102*, 9983–9999. [CrossRef]
14. Encyclopædia Britannica. Aleppo Earthquake of 1138. Available online: https://www.britannica.com/event/Aleppo-earthquake-of-1138 (accessed on 26 April 2023).
15. Darawcheh, R.; Abdul-wahed, M.K.; Hasan, A. The 13th-August-1822 Aleppo Earthquake: Implications for the Seismic Hazard Assessment at the Antakia Triple Junction. In *On Significant Applications of Geophysical Methods. CAJG 2018. Advances in Science, Technology & Innovation*; Sundararajan, N., Eshagh, M., Saibi, H., Meghraoui, M., Al-Garni, M., Giroux, B., Eds.; Springer: Cham, Switzerland, 2019. [CrossRef]
16. Lekkas, E.; Carydis, P.; Vassilakis, E.; Mavroulis, S.; Argyropoulos, I.; Sarantopoulou, A.; Mavrouli, M.; Konsolaki, A.; Gogou, M.; Katsetsiadou, K.N.; et al. The 6 February 6 2023 Turkey-Syria Earthquakes. In *Newsletter of Environmental, Disaster and Crises Management Strategies*; National and Kapodistrian University of Athens: Athens, Greece, 2023; p. 29, ISSN 2653-9454. [CrossRef]
17. British Geological Survey. The Kahraman Maraş Earthquake Sequence, Turkey/Syria. Available online: https://www.bgs.ac.uk/news/the-kahraman-maras-earthquake-sequence-turkey-syria/ (accessed on 5 March 2023).
18. Citypopulation. Population Statistics, Charts and Map. Available online: https://www.citypopulation.de/en/turkey/admin/ (accessed on 3 March 2023).
19. Encyclopædia Britannica. Kahramanmaraş. Available online: https://www.britannica.com/place/Kahramanmaras (accessed on 3 March 2023).
20. GSNL. Kahramanmaraş Event Supersite. Available online: https://geo-gsnl.org/supersites/event-supersites/active-event-supersites/kahramanmaras-event-supersite/ (accessed on 9 June 2023).
21. European-Mediterranean Seismological Centre. Available online: https://www.emsc-csem.org/#2 (accessed on 16 May 2023).
22. ESA. Sentinel-2 Overview. Available online: https://sentinel.esa.int/web/sentinel/missions/sentinel-2/overview (accessed on 5 March 2023).
23. ESA. Sentinel-2 Product Types. Available online: https://sentinel.esa.int/web/sentinel/user-guides/sentinel-2-msi/product-types (accessed on 5 March 2023).
24. ESA. Sentinel Online, Level-2A Product. Available online: https://sentinel.esa.int/web/sentinel/user-guides/sentinel-2-msi/product-types/level-2a (accessed on 5 March 2023).
25. Meteostat. Gaziantep | Weather History & Climate. Available online: https://meteostat.net/en/station/17260?t=2023-01-25/2023-02-09 (accessed on 9 June 2023).
26. Meteostat. Kahramanmaras | Weather History & Climate. Available online: https://meteostat.net/en/station/17255?t=2023-01-25/2023-02-09 (accessed on 9 June 2023).
27. Copernicus. Copernicus Emergency Management Service–Mapping. Available online: https://emergency.copernicus.eu/mapping/copernicus-emergency-management-service#zoom=4&lat=33.51964&lon=44.12109&layers=0BT00 (accessed on 5 March 2023).
28. Uhe, P.; Hawker, L.; Paulo, L.; Sosa, J.; Sampson, C.; Neal, J. FABDEM-A 30m Global Map of Elevation with Forests and Buildings Removed. In Proceedings of the EGU General Assembly 2022, Vienna, Austria, 23–27 May 2022. [CrossRef]
29. ForM@Ter–EOST. Terrain Displacement from the Turkiye-Syria Earthquakes of February 6, 2023 Obtained with the GDM-OPT-ETQ Service Applied on Sentinel-2 Optical Imagery; ForM@Ter–EOST: 2023. Available online: https://doi.data-terra.u-strasbg.fr/GDM_OPT_Turkey_Syria/ (accessed on 9 June 2023).
30. Ou, Q.; Lazecky, M.; Watson, C.S.; Maghsoudi, Y.; Wright, T. *3D Displacements and Strain from the 2023 February Turkey Earthquakes, Version 1*; NERC EDS Centre for Environmental Data Analysis: Didcot, UK, 2023. [CrossRef]